ANALYSIS OF ACHIEVABLE DISTURBANCE ATTENUATION IN A PRECISION MAGNETICALLY-SUSPENDED MOTION CONTROL SYSTEM

Alexander V. Kuzin, Michael L. Holmes, Roxana Behrouzjou, David L. Trumper

Department of Electrical Engineering, University of N. Carolina at Charlotte,
Charlotte, NC 28223 USA

SUMMARY

The results of the analysis of the achievable disturbance attenuation to get an Angstrom motion control resolution and macroscopic travel in a precision magnetically-suspended motion control system are presented in this paper. Noise sources in the transducers, electronics, and mechanical vibrations are used to develop the control design.

INTRODUCTION

Precision motion control at the nanometer level is required in many potential applications, e.g., for semiconductor manufacturing, large-travel probe microscopy, probing and analysis of integrated-circuit structures, and the testing of micromachines. Magnetic suspension makes possible performance of precision motion control systems which can not be achieved by other means [1]. An important requirement in precision motion control systems with magnetic suspension is that the disturbance influence on control coordinates of motion should be below a given value. There are fundamental trade-offs between the conflicting objectives of reducing sensitivity to disturbances (mechanical vibrations) and parameter uncertainty on the one hand, and filtering out any internally generated noise (sensor noise) on the other. It is the existence of these trade-offs which makes control system design for fine-motion control systems difficult. This paper deals with analysis of achievable disturbance attenuation in precision magnetically-suspended motion control systems. The objective is to get an Angstrom resolution in a 100 μm cube of accessible travel of the suspended platen.

DESCRIPTION OF THE SYSTEM

The magnetically-suspended six-degree-of-freedom motion control stage will be floated in oil to support its weight, provide mechanical damping, and high-frequency coupling [2]. In one possible design, the platen is suspended by a symmetric arrangement of twelve electromagnets $M1 - M12$ (Fig.1). The electromagnets are mounted in the machine frame and act on ferromagnetic targets

mounted in the platen. These electromagnets are arranged symmetrically at the corners of the platen. Since the electromagnets can exert only attractive forces, the actuators are arranged in pairs on opposite faces of the platen. The capacitance probes $C1 - C6$ provide measurement of the coordinates of the platen.

Magnet Force Measurements

In order to design a control system for the purpose of achieving levitation of the platen, accurate measurements of the magnet force characteristics were made. To carry out these measurements, the magnetic bearing calibration fixture has been used with the following characteristics [3]: measurement of the electromagnet actuator force from minimum to maximum core flux density at separation gaps ranging from 10 to 1000 microns; peak force capability on the order of hundreds of newtons; adjustment of the target separation gap as well as the rotation of the target relative to the actuator.

To study the magnetic force dependence of angle position of the platen, the measurements of magnetic force for maximum possible platen rotation about the short and long axis of the electromagnet were made. According to the magnet force measurements, it was accepted that in the first approach we can neglect the influence of rotation on the force characteristics of the electromagnets. The force of each electromagnet is the function of current of the electromagnet i_i and the gap between the surface of the electromagnet and platen target q_i

$$F_{m_i} = k_{i_i} i_i - k_{q_i} q_i, \qquad (1)$$
$$i = 1, ..., 6.$$

The negative sign in the formula shows that the magnetic force decreases when gap increases.

Fluid damping

The platen will be floated in low-vapor-pressure viscous oil in order to support its weight and thus minimize power dissipation. The oil flotation provides several advantages. First, oil increases the high-frequency coupling between the platen and the frame. At frequencies above those which are well controlled by the active suspension, the platen motions are controlled through viscous coupling to the frame. Second, the oil supplies viscous damping to platen and frame vibrations and resonances. Such resonances can be troubling for ultra-precision control systems, and it is far better to solve them in the mechanical domain rather than attempting to compensate for them in the feedback controller domain. There are two kinds of damping influence from the fluid to the floated moving platen. The first one is the force of inertial friction of the fluid or its resistance to shear. This force is propotional to the contact area of the two separate surfaces, the speed of relative motion, and inversely proportional to the distance separating the two surfaces having the relative motion.

$$F_{d1} = \mu A \frac{v}{q}, \tag{2}$$

where μ - viscosity of fluid; A - area; q - separating distance; v - speed of movement. The second one is the squeeze film damping force. The load-carrying phenomenon arises from the fact that a viscous lubricant cannot be instantaneously squeezed out from between two surfaces that are approaching each other. It takes time for these surfaces to meet and during that interval, because of the lubricant's resistance to extrusion, a pressure is built up and the load is actually supported by the oil film. If the load is applied for a short enough period, it may happen that the two surfaces will not meet at all. According to the design (Fig.1), the nearest distance between the platen and the frame is the distance between the surfaces of the capacitive sensors and their targets on the platen. For one capacitive probe we have the case of a single circular plate of radius R approaching a flat plate. For this case the damping force F_d is [4]

$$F_{d2} = \frac{3\pi\mu R^4 v}{2q^3}. \tag{3}$$

The comparison of the equations (2) and (3) shows that the squeeze film damping force is much greater than the shearing damping force and therefore, we can neglect the latter in the calculations. Formula (3) allows us to estimate the desirable forces of electromagnets which they have to provide for movement of the platen along the corresponding coordinate.

The results of the damping force calculations allow us to make the conclusion that due to the large mechanical damping, which we can control through the choice of the fluid viscosity, area of the contacting surfaces and the distance between the contacting surfaces, we do not need additional electrical damping implemented in the controller design. So, to control the platen motion we can use the simple proportional controller.

Development of model for system dynamics

According to the equations for magnetic forces and moments we have the following model for system dynamics

$$m\ddot{x} + b_x\dot{x} - 3k_q x = F_{x_{dist}} + k_i(i_1 + i_2 + i_3); \tag{4}$$

$$m\ddot{y} + b_y\dot{y} - 2k_q y = F_{y_{dist}} + k_i(i_4 + i_5); \tag{5}$$

$$m\ddot{z} + b_z\dot{z} - k_q z = F_{z_{dist}} + k_i i_6; \tag{6}$$

$$J_x\ddot{\gamma} + b_\gamma\dot{\gamma} - 2L^2 k_q \gamma = M_{x_{dist}} + Lk_i(i_5 - i_4); \tag{7}$$

$$J_y\ddot{\psi} + b_\psi\dot{\psi} - \frac{3L^2}{2}k_q\psi = M_{y_{dist}} + Lk_i[i_1 - \frac{1}{2}(i_2 + i_3)]; \tag{8}$$

$$J_z\ddot{\theta} + b_\theta\dot{\theta} - \sqrt{3}L^2 k_q\theta = M_{z_{dist}} + Lk_i(i_3 - i_2); \tag{9}$$

where m - mass of platen; J_x, J_y, J_z - inertia moments of platen about axes x, y, z; $\ddot{x}$, $\ddot{y}$, $\ddot{z}$, $\ddot{\gamma}$, $\ddot{\psi}$, $\ddot{\theta}$ - accelerations of the platen along corresponding coordinate; $F_{i_{dist}}$ - disturbance force ; $M_{i_{dist}}$ -

disturbance moment; b_i, $(i = x, y, z, \gamma, \psi, \theta)$ - damping coefficients along corresponding coordinate i; $\dot{x}$, $\dot{y}$, $\dot{z}$, $\dot{\gamma}$, $\dot{\psi}$, $\dot{\theta}$ - velocities of the platen along of corresponding coordinate. The previous equations show that in the first approach we can use the equation for each coordinate independently of the other coordinates and design the controller only for this coordinate.

CONTROL SYSTEM DESIGN

An important requirement in precision motion control systems with magnetic suspension is that the disturbance influence on control coordinates of motion should be below a given value.To provide low-noise control system design, the analysis of disturbances and their mathematical models are necessary. The system under consideration is shown in Fig.2, where P and C are the plant and controller transfer functions. The signals in the system are as follows: r - reference or command signal; e - tracking error; u - control signal, controller output; f - plant disturbance; x - plant output; s - sensor noise.

Analysis and mathematical model of disturbances

The main disturbances in the system are mechanical vibrations of the frame and sensor noise. To analyze the mechanical vibration disturbance, the measurements of the floor vibrations using a Wilcoxon research seismic accelerometer, model 731, and a DT-2823 data acquisition board for a PC-computer were used. The measured signal of vibration acceleration is presented in the Fig.3. The histogram of the measured vibration acceleration signal shows that signal amplitudes follow a Gaussian probability distribution with a mean of zero (Fig.4). For a Gaussian distribution there is correlation between standard deviation or root-mean-square (RMS) value and peak-to-peak value which is shown in Table 1. This correlation allows an estimate of the peak-to-peak value of random process if the RMS value is known. To analyze the spectral range, the spectrum of vibrations was measured using HP-35665A dynamic signal analyzer. This spectrum showed that the spectral range of vibrations is inside the 0 - 35 Hz region. Therefore, we can accept that vibration disturbance is the white noise with some spectral density which goes through the low-pass filter with the noise bandwidth equal to 35 Hz. According to this mathematical model the vibration signal looks as white noise with spectral density $S_f(\omega) = 1.41 \cdot 10^{-9} \frac{N^2}{sec}$ which goes through a first-order low-pass filter with a transfer function

$$W_1(s) = \frac{1}{T_1 s + 1}, \tag{10}$$

where $T_1 = .0071 sec.$
The graph of the imitation signal of vibration and the histogram of the imitation signal are shown in Fig.3 and Fig.4 respectively and show good coincidence between real and imitation signals. The analogous method was used for the design of the mathematical model of the sensor noise. Similarly, the sensor noise looks as the white noise with spectral density $S_s(\omega) = 3.33 \cdot 10^{-13} \frac{V^2}{sec}$ which goes through a first-order low-pass filter with a transfer function

$$W_2(s) = \frac{1}{T_2 s + 1}, \tag{11}$$

where $T_2 = .00025sec.$

For noise and error amplitudes which follow a Gaussian (normal) probability distribution with a mean of zero, the mean square value equals the variance σ^2 of the output error signal and RMS equals the standard deviation σ. Mean square error σ^2 for our system looks as follows:

$$\sigma^2 = \frac{1}{2\pi}\int_{-\infty}^{\infty} |\frac{P(j\omega)}{1 + P(j\omega)C(j\omega)}|^2 S_f(\omega)d\omega + \frac{1}{2\pi}\int_{-\infty}^{\infty} |\frac{P(j\omega)C(j\omega)}{1 + P(j\omega)C(j\omega)}|^2 S_s(\omega)d\omega. \tag{12}$$

Our control problem may be formulated as follows. Assuming that the noise and the disturbance are the stationary random functions having known correlation functions or spectral densities, it is required for known structure of the controller to find the parameters which would provide the stability of a closed-loop system and minimize noise level of the output signal.

Analysis of One-Degree-of-Freedom System

According to the previous conclusions we can analyze the dynamics of our system for each coordinate independently. So, let us analyze the one-degree-of-freedom system corresponding to vertical linear motion of the platen. The system under consideration is shown in Fig.5. In this case the equation of the movement of the platen looks as follows:

$$m\ddot{x} + b_x\dot{x} - k_x x = F_{dist} - k_i i, \tag{13}$$

where $F_{dist} = -m\ddot{x}_f$ - disturbance force, caused by the vibrations of the frame relative to inertial space; $F_d = -b_x\dot{x}$ - damping force; $F_m = k_i i - k_x x$ - force of electromagnet; $x_m = x_f + x$, $\ddot{x}_m = \ddot{x}_f + \ddot{x}$; x_m is the coordinate of the platen relative to the inertial space, x_f is the coordinate of the frame relative to the inertial space, and x is the gap between the electromagnet and platen which it is necessary to stabilize during the functioning of the control system. To make the system closed-loop we need to add to the equation of motion (13) the equation of the x position sensor of the platen

$$u_s = k_s x, \tag{14}$$

where u_s - output voltage of sensor; k_s - proportional coefficient which represents transformation of displacement into sensor output voltage; and the equation of controller which transforms output voltage of sensor into control current of electromagnet with some proportional coefficient k_c:

$$i = k_c x. \tag{15}$$

Equation for variance σ_x^2 of the output signal looks as follows

$$\sigma_x^2 = \sigma_{xf}^2 + \sigma_{xs}^2 \tag{16}$$

$$= \frac{1}{2\pi}\int_{-\infty}^{\infty} |\frac{1}{m(j\omega)^2 + b_x(j\omega) + (k_i k_c k_s - k_x)} W_1(j\omega)|^2 S_f(\omega)d\omega$$

$$+\frac{1}{2\pi}\int_{-\infty}^{\infty}|\frac{k_ik_c}{m(j\omega)^2+b_x(j\omega)+(k_ik_ck_s-k_x)}W_2(j\omega)|^2S_s(\omega)d\omega$$

$$=\frac{T_1(b_xT_1+1)}{2(k_ik_ck_s-k_x)T_1((b_xT_1+1)(k_ik_ck_sT_1+b_x-k_xT_1)-(k_ik_ck_s-k_x)T_1))}S_f(\omega)$$

$$+\frac{T_2(k_ik_c)^2(b_xT_2+1)}{2(k_ik_ck_s-k_x)T_2((b_xT_2+1)(k_ik_ck_sT_2+b_x-k_xT_2)-(k_ik_ck_s-k_x)T_2))}S_s(\omega).$$

Equation (16) is of great importance, because it allows us to solve the problem of trade-offs between the conflicting objectives of reducing sensitivity to mechanical vibrations and filtering out the sensor noise. We can evaluate the value of the variance and, therefore, the peak-to-peak deviation of the output signal in relation with the parameters of the system and choose these parameters in accordance with the required peak-to-peak deviation of output signal and system's bandwidth. The first integral in equation (16) is decreasing with increasing coefficient k_c of the controller and the second one is increasing in this case. This is clear if the time constants T_1 and T_2 in equation (16) are equal to zero. Fig.6 represents the graph of dependence of the first and second integrals in (16) and their sum of controller coefficient. Therefore, the equation for mean square of output signal deviation has the extreme value (in particular, a minimum) and we can find this coefficient of the controller which produces this minimum. The predicted, according to correlation,

$$PP_x = 8 \cdot \sigma_x \tag{17}$$

peak-to-peak deviation of x coordinate and peak-to-peak deviation from simulation results for different controller and damping coefficients are shown in Fig.7. The results of Fig.7 show that for controller coefficients above 20 $[\frac{A}{V}]$ (system bandwidth above 20 $[\frac{rad}{sec}]$), the sensor noise dominates and we can neglect the influence of the vibration acceleration noise. The typical sensor noise and simulated error motions of the oil floated stage under closed loop control are shown in Fig. 8. The pure proportional controller reduces the system sensitivity to noise and we can get Angstrom-scale stability of the closed-loop system.

Correlation of the parameters of the system and bandwidth

To analyze the correlation of the system parameters and bandwidth we can roughly define the bandwidth ω_b of our control system as cross-over frequency and find it as frequency ω_c for which $|P(j\omega)C(j\omega)| \cong |(\frac{k_ck_mk_s}{k_dm})/(j\omega - \frac{k_x}{k_d})| = 1$

$$\omega_c = \sqrt{\frac{k_c^2k_m^2k_s^2 - k_x^2m^2}{k_d^2m^2}} \cong \frac{k_ck_mk_s}{k_dm} \cong \omega_b. \tag{18}$$

For parameters of the system: $k_m = 3.33N/A$; $k_s = 2 \cdot 10^5 v/m$; $m = 1kg$

$$\omega_b = 6.66 \cdot 10^5 \frac{k_c}{k_d}.$$

The points of different bandwidth are shown in Fig.7.

Simulation of asymptotic tracking

To evaluate the correspondance of the designed control system to the required objective of a 100 μm accessible travel, the simulation of asymptotic tracking of the platen in vertical direction was made. The nonlinear dependence of the damping force from the separation gap according to equation (3) was used in the simulation. The results of simulation are shown in Fig. 9, where the force equals the sum of forces of three pairs of vertical electromagnets (Fig.1) and current equals the sum of currents in those electromagnets. The results of the simulation show that the control system provides required asymptotic tracking of a reference signal and an acceptable level of the currents in electromagnets.

CONCLUSIONS

Experimental measurements of the accelerations in laboratory and the noise of real capacitive probes combined with the statistical approach to the design of the control system and simulation of the system under closed-loop control indicate that the required peak-to-peak deviations of the platen coordinates and system's bandwidth can be achieved through the appropriate choosing of the proportional controller coefficients, fluid film damping coefficients, and appropriate sensor noise filtering. Thus the stage should be capable of operating to its specified resolution in common laboratory environments without the need for any special vibration isolation devices.

A hardware prototype of a precision magnetically-suspended six-degree-of-freedom motion control stage with Angstrom resolution is now under construction, allowing experimental verification of the performance which has been analytically predicted.

REFERENCES

1. Trumper, D.L.: Magnetic Suspension Techniques for Precision Motion Control, Ph.D. Thesis, Dept. of Elec. Eng. and Comp. Sci., M.I.T., Camb., Massachusetts, 1990.
2. Trumper, D.L.: Analysis and Design of a Viscously-Damped Magnetic Suspension System. Proceedings of the 1993 NSF Design and Manufacturing Systems Conference, vol.2, January 6-8, 1993.
3. Poovey, T., M. Holmes, D. Trumper: A Kinematically Coupled Magnetic Bearing Calibration Fixture, Accepted for publication in *Precision Engineering Journal*, 1993.
4. Fuller, D. D.: *Theory and Practice of Lubrication for Engineers*, A Wiley-Interscience Publication, JOHN WILEY&SONS, 1984.
5. Solodovnikov, V.V.: *Statistical Dynamics of Linear Automatic Control Systems*, London: D. Van Nostrand Company, LTD, 1965.

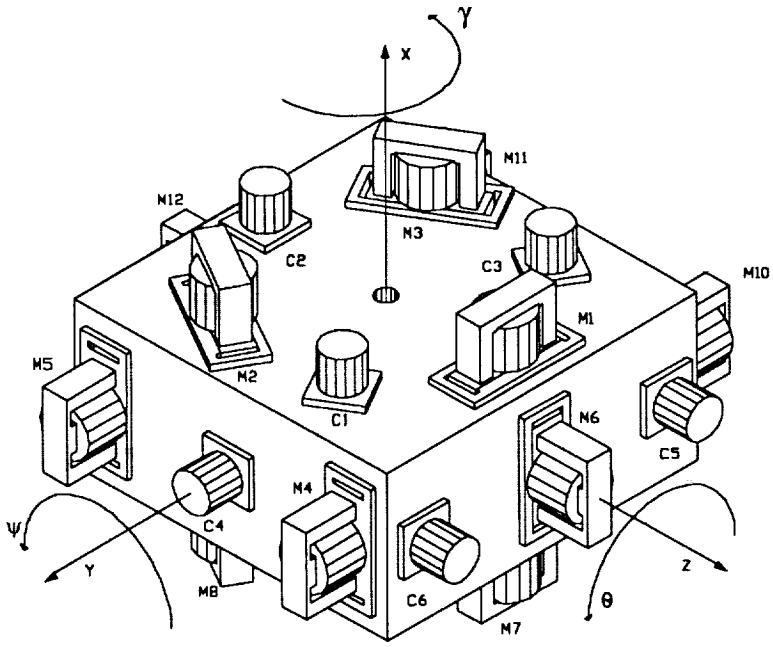

Figure 1: Schematical system design

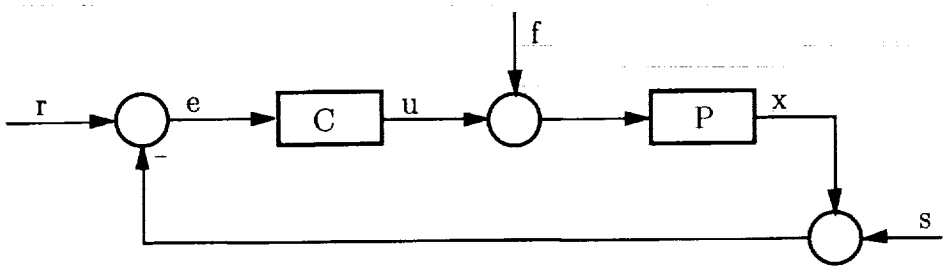

Figure 2: Scheme of general system

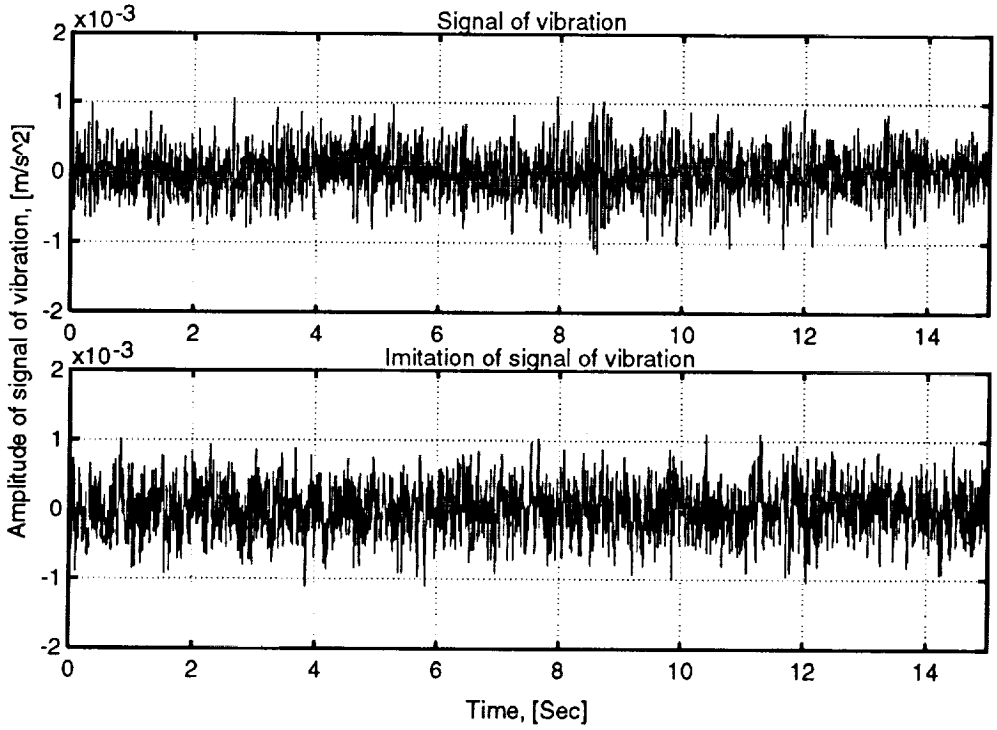

Figure 3: Signal of vibration and its imitation

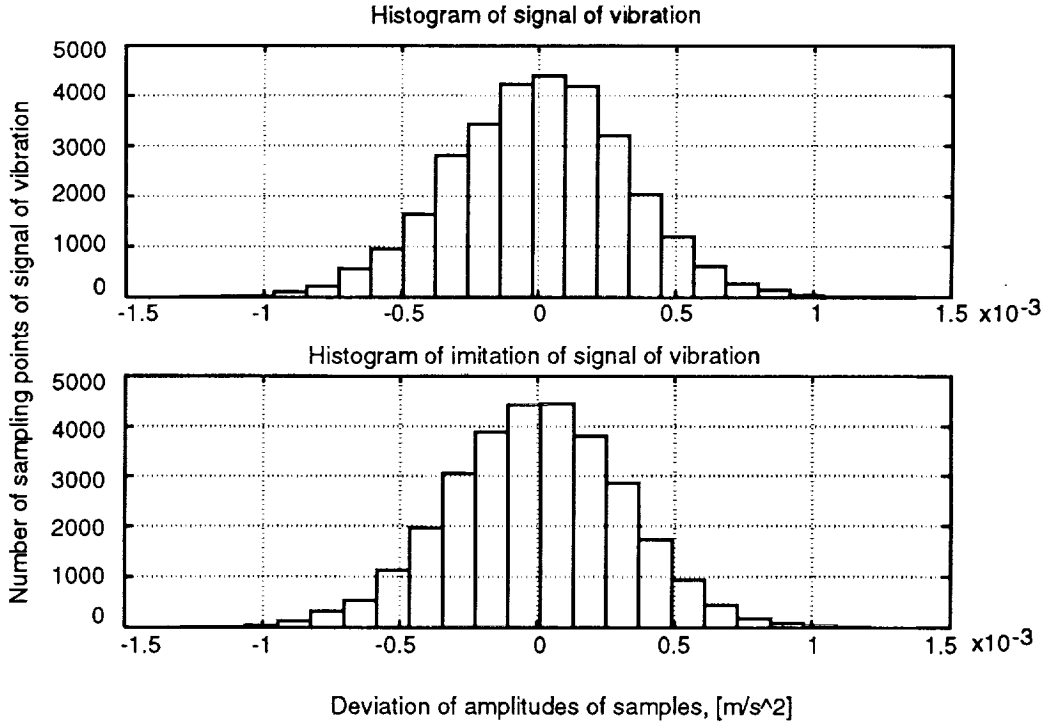

Figure 4: Histograms of signal of vibration and their imitation

Table 1: Correlation between peak-to-peak and RMS values for Gaussian random processes

Peak-to-peak value, N σ N=1..8; σ- standard deviation(RMS)	Probability of appearance of amplitudes, greater then N σ
1 σ	32%
3 σ	13%
4 σ	4.6%
5 σ	1.2%
6 σ	.27%
7 σ	.047%
8 σ	.0063%

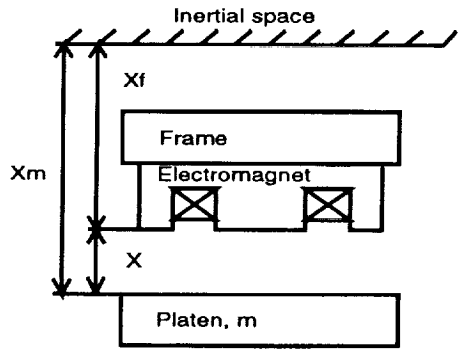

Figure 5: Scheme of the system

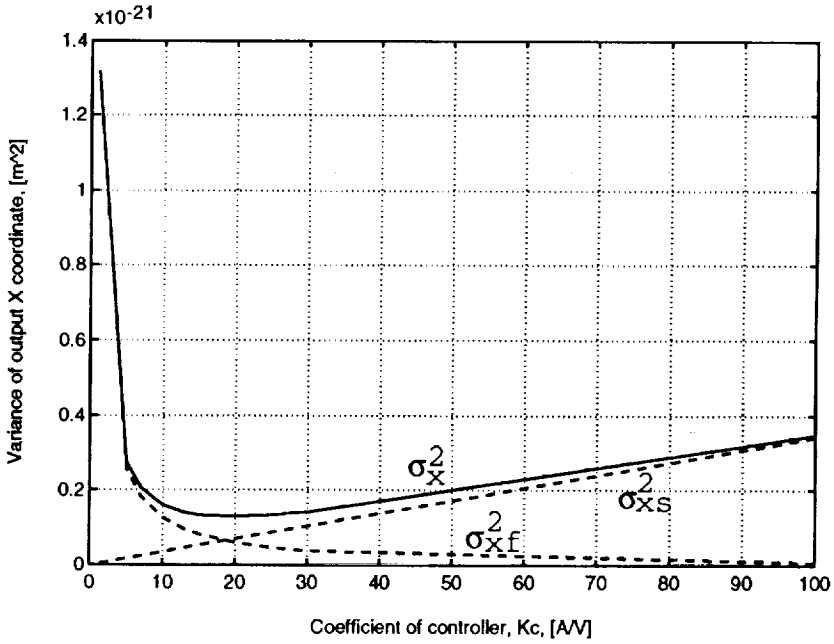

Figure 6: Dependence of the output signal variance of the controller coefficient

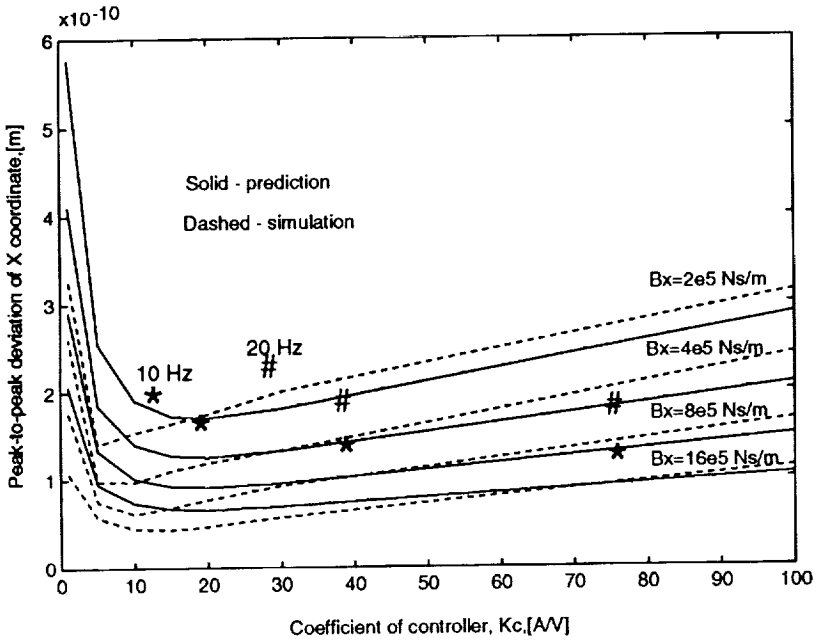

Figure 7: Peak-to-peak deviation

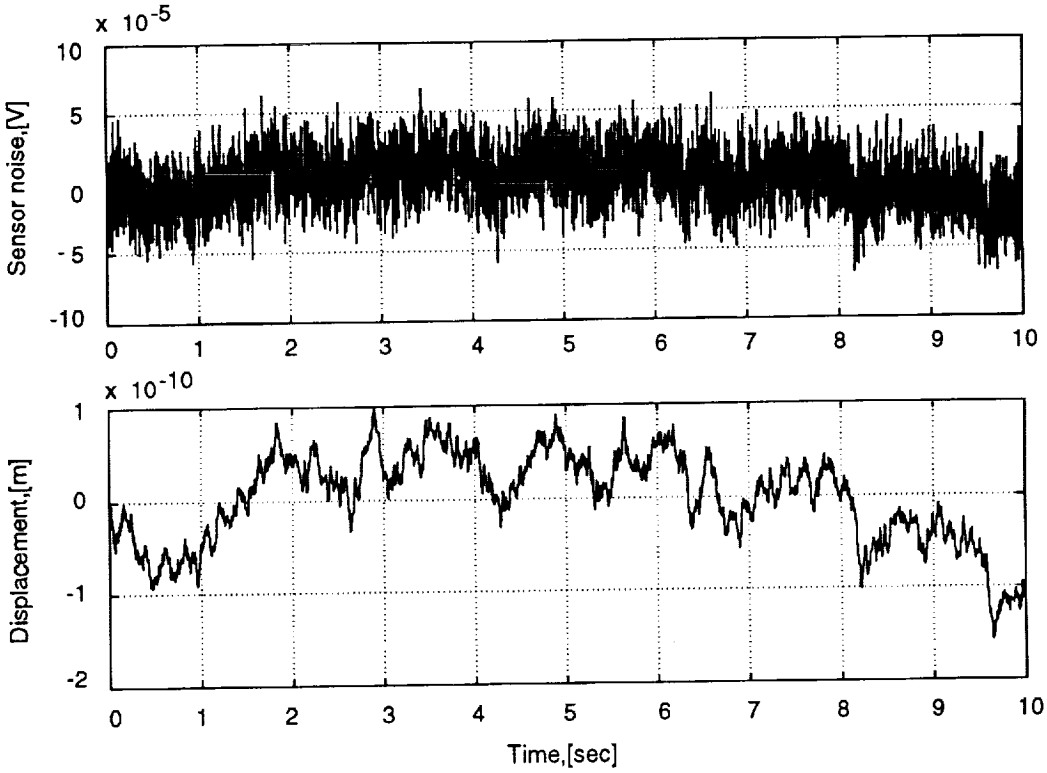

Figure 8: Typical sensor noise and simulated error motions

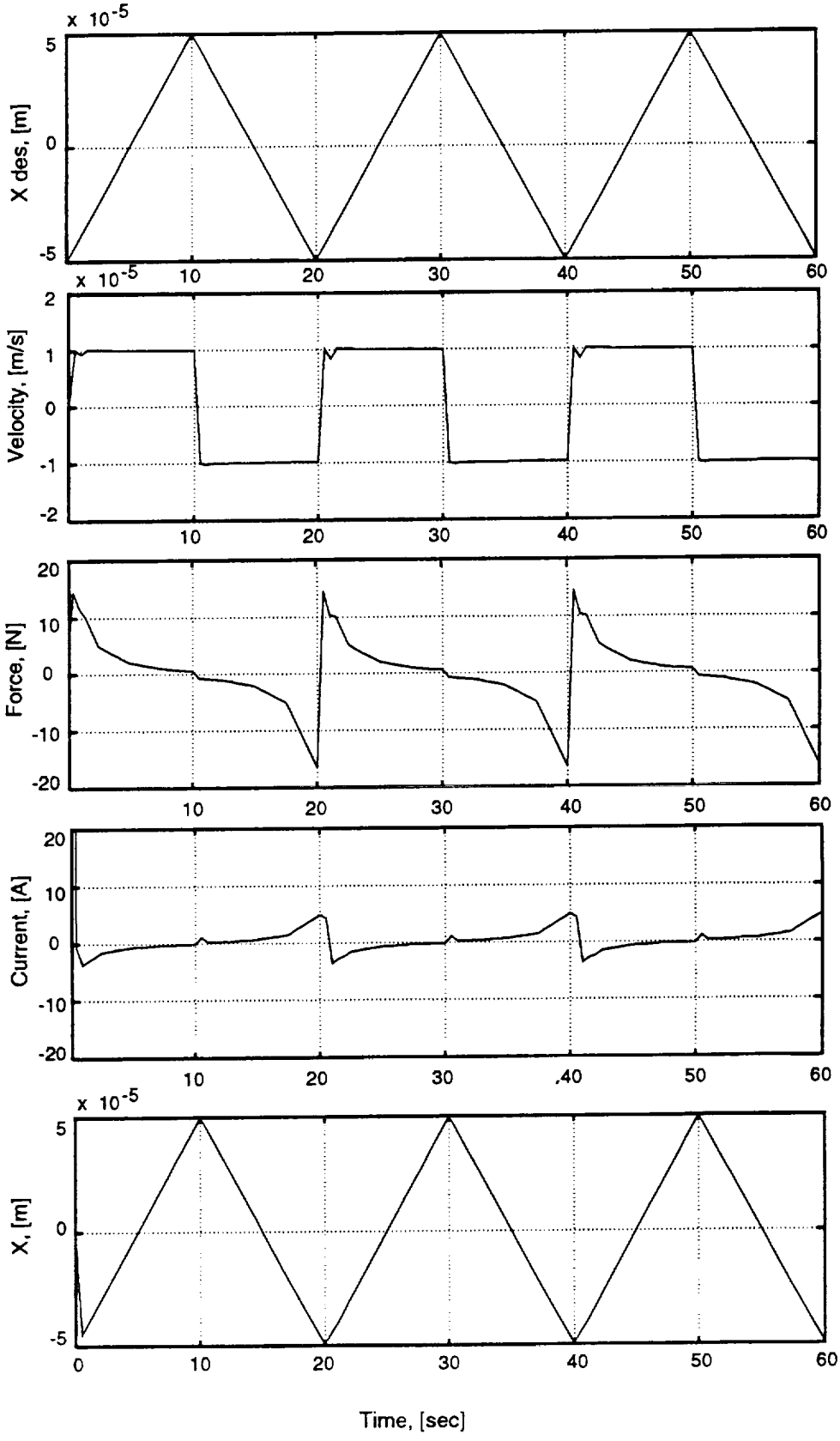

Figure 9: Simulation of asymptotic tracking